Driver-Automation Cooperative Approach for Shared Steering Control Under Multiple System Constraints: Design and Experiments

Tran Anh-Tu Nguyen, Chouki Sentouh, Jean-Christophe Popieul

▶ **To cite this version:**

Tran Anh-Tu Nguyen, Chouki Sentouh, Jean-Christophe Popieul. Driver-Automation Cooperative Approach for Shared Steering Control Under Multiple System Constraints: Design and Experiments. IEEE Transactions on Industrial Electronics, 2017, 64 (5), pp.3819-3830. 10.1109/TIE.2016.2645146 . hal-03428784

HAL Id: hal-03428784
https://uphf.hal.science/hal-03428784

Submitted on 25 Nov 2023

HAL is a multi-disciplinary open access archive for the deposit and dissemination of scientific research documents, whether they are published or not. The documents may come from teaching and research institutions in France or abroad, or from public or private research centers.

L'archive ouverte pluridisciplinaire **HAL**, est destinée au dépôt et à la diffusion de documents scientifiques de niveau recherche, publiés ou non, émanant des établissements d'enseignement et de recherche français ou étrangers, des laboratoires publics ou privés.

ResearchGate

See discussions, stats, and author profiles for this publication at: https://www.researchgate.net/publication/311973031

Driver–Automation Cooperative Approach for Shared Steering Control Under Multiple System Constraints: Design and Experiments

Article *in* IEEE Transactions on Industrial Electronics · May 2017

DOI: 10.1109/TIE.2016.2645146

CITATIONS
156

READS
1,269

3 authors, including:

Anh-Tu Nguyen
Université Polytechnique Hauts-de-France
140 PUBLICATIONS **2,084** CITATIONS

SEE PROFILE

Chouki Sentouh
LAMIH UMR CNRS 8201 Hauts-de-France Polytechnic University
114 PUBLICATIONS **2,057** CITATIONS

SEE PROFILE

All content following this page was uploaded by Anh-Tu Nguyen on 12 October 2017.

The user has requested enhancement of the downloaded file.

Driver-Automation Cooperative Approach for Shared Steering Control under Multiple System Constraints: Design and Experiments

Anh-Tu Nguyen, Chouki Sentouh, and Jean-Christophe Popieul

***Abstract*—This paper addresses the shared lateral control between a human driver and a lane keeping assist system of intelligent vehicles for both lane keeping and obstacle avoidance. This control issue is very challenging in today's automotive industry due to the human-machine interaction involved in the control design. In this work, we propose a new approach to consider such an interaction via a fictive driver activity parameter introduced into the road-vehicle system. Hence, the steering assistance actions can be computed according to the driver's real-time behaviors. Takagi-Sugeno fuzzy control approach is proposed to deal with the time-varying driver activity parameter and vehicle speed. Especially, the concept of robust invariant set is exploited using Lyapunov arguments to handle theoretically both system state and control input limitations. Considering these system constraints in the control design procedure aims to improve the driver's safety and comfort. Experimental tests with a human driver and an advanced interactive dynamic driving simulator are conducted to show the effectiveness of the proposed method.**

***Index Terms*—Human-in-the-loop control, human-machine shared control, linear matrix inequality (LMI), Lyapunov-based control, steering assistance system, Takagi-Sugeno fuzzy control.**

I. Introduction

NOWADAYS, most of modern vehicles are equipped with steering assistance systems which can assist the driver in various driving situations [1], [2]. It has been shown that these systems contribute to reduce significantly the driver workload and also road accidents [3]. Therefore, the control design of intelligent vehicle systems has attracted increasing attention from both academic and industrial researchers [3]–[6].

The introduction of a steering assistance system into the vehicle implies crucial impacts on the driving process [2]. Indeed, this system can modify the driver's activity and also eventual risks coming from the external environment [2]. For example, the complex interaction between a human driver and an active front steering system has been well discussed in [7]. Hence, in many driving situations the conflict issue (i.e. when the driver and the automation do not have the same driving objectives) may arise. To avoid conflict situations, shared control considering the human-machine interaction has recently appeared as a promising solution [8]–[10]. The goal of such a control approach is to allow both human driver and automation system being able to exert *simultaneously* and *appropriately* the control actions on the steering wheel [9], [11]. In this way, the automation does not prevent the human to perform some specific tasks that have not been detected by the automation or, even better, the automation should help him/her to realize these maneuvers. Up to now, human-machine shared control approach has been investigated for a wide range of applications such as automotive control [11], UAV teleoperation [12], robotics control [13]. Recent works [8]–[10] have also shown that the integration of driver's behaviors (based on measurements and modeling) into the control loop provides a better management of driver-automation conflict. Especially, the automation should have an *appropriate* control authority allocation to allow the driver to disagree, or fully take the vehicle control in case of necessity.

This paper addresses the control design of a lane keeping assist system (LKAS) of intelligent vehicles. Aiming to improve the safety and comfort, this kind of assistance devices can actively share the vehicle steering control with human drivers [2]. Through the steering wheel, the human driver can directly feel the actions provided by the assistance system and s/he can immediately understand if these actions are suitable to a given driving situation or not. As a result, there is a clear intrusion of automation on the driver's steering activity. Notice also that the driver always decides on the vehicle trajectory in case of disagreement between two driving actors. Shared lateral control of LKAS with an effective management of driver-automation conflict is known as a challenging issue in today's automotive industry [11]. In [9], based on an $\mathcal{H}_2-$preview optimization problem, the authors have presented a cooperative controller for only lane keeping task which can share the control authority with the driver. Another shared lateral controller has been proposed in [10] to deal with both lane keeping and obstacle avoidance. In that work, the degree of cooperation between two driving actors is quantified by a linear quadratic

Manuscript received May 19, 2016; revised August 3, 2016 and October 14, 2016; accepted November 19, 2016. This work was done in the framework of the CoCoVeA research program (ANR-13-TDMO-0005), funded by the National Research Agency. This work was also sponsored by the International Campus on Safety and Intermodality in Transportation, the Hauts-de-France Region, the European Community, the Regional Delegation for Research and Technology, the Ministry of Higher Education and Research, the French National Center for Scientific Research.

A.-T. Nguyen, C. Sentouh and J.-C. Popieul are with the Control Department, LAMIH UMR CNRS 8201, University of Valenciennes, France (e-mails: nguyen.trananhtu@gmail.com, chouki.sentouh@univ-valenciennes.fr, jean-christophe.popieul@univ-valenciennes.fr).

(LQ) criterion to be minimized. Notice that in both [9] and [10] the designed steering assistance actions cannot exploit the real-time information on the driver's behaviors and also his/her driving state coming from the driver monitoring system [5]. Moreover, it seems hard to tune the weighting matrices in the LQ criterion in [10] to manage effectively the conflict issue for a general driving situation. In this work, we take a step further to design a new controller for vehicle shared lateral control problem which can overcome these drawbacks. To do that, a time-varying parameter representing the real-time activity of the driver will be judiciously introduced into the road-vehicle system. Considering directly this information in the control design can provide an effective solution to manage the driver-automation conflict issue.

Over the last decade, Takagi-Sugeno (T-S) fuzzy model-based methods [14] have been received a great deal of attention in both control theory and applications [15]–[20]. This is due to the fact that T-S fuzzy control can provide a systematic design framework for nonlinear and/or linear parameter-varying (LPV) systems [14], [21]. In this work, T-S fuzzy control approach will be proved as a powerful tool to deal with the time-varying driver activity variable and vehicle speed. Notice that although considering the variation of vehicle speed in the control design allows to improve the control performance and the driver-automation coordination in various driving circumstances [10], this is however neglected in most of existing works. In particular, motivated by our real-world application, both system state and control input constraints are *theoretically* handled using Lyapunov arguments to improve the driver's safety and comfort [4]. Note also that in many specific driving maneuvers, for instance lane change or obstacle avoidance, the assistance torque may tend to be saturated to compensate an important torque received from the driver. Therefore, the input saturation should be *explicitly* considered to prevent the loss of stability, especially when disturbances are involved in the system dynamics [22]. The main contributions of this paper are summarized as follows.

1) A new shared control approach for LKAS devices with an *adaptive* control authority allocation between the driver and the automation is proposed. This approach includes the driver's real-time driving activity into the control design and offers an effective solution for the shared control issue.
2) Based on the concept of robust invariant set [23], a new control method for T-S systems subject to both state and control input limitations is derived. In particular, the closed-loop T-S fuzzy system is *equivalently* rewritten in an augmented form for the derivation of LMI (linear matrix inequality [24]) based design conditions. This allows the use of a special parameter-dependent Lyapunov function with slack decision variables to reduce the design conservatism. The proposed T-S control method can be also applied to a large class of constrained nonlinear/LPV systems.
3) The proposed theoretical results and the new shared control approach have been successfully validated with a human driver and an advanced dynamic driving simulator.

The paper is organized as follows. Section II presents the driver-vehicle system. In Section III, the proposed shared control strategy is described. A new Lyapunov-based control method for constrained T-S systems is developed in Section IV. Section V highlights the application of the proposed method to the shared lateral control issue. Experimental results are reported in Section VI and Section VII concludes the paper.

II. Modeling for Shared Lateral Control

This section reviews the driver-vehicle modeling for lateral control purposes. The vehicle parameters are given in Table I.

A. Road-Vehicle Model with Steering Assistance System

In this work, since we focus on the shared lateral control, the well-known bicycle model [3] is used to represent the vehicle lateral dynamics, see Fig. 1. Then, the vehicle system integrating the electric power steering model can be described as follows [3], [4], [9]:

$$\dot{x}_v = Ax_v + B\left(T_c + T_d\right) + B_w w, \tag{1}$$

where

$$A = \begin{bmatrix} a_{11} & a_{12} & 0 & 0 & b_1 & 0 \\ a_{21} & a_{22} & 0 & 0 & b_2 & 0 \\ 0 & 1 & 0 & 0 & 0 & 0 \\ 1 & l_s & v_x & 0 & 0 & 0 \\ 0 & 0 & 0 & 0 & 0 & 1 \\ T_{s1} & T_{s2} & 0 & 0 & T_{s3} & T_{s4} \end{bmatrix},\ B = \begin{bmatrix} 0 \\ 0 \\ 0 \\ 0 \\ 0 \\ \lambda \end{bmatrix},\ B_w = \begin{bmatrix} e_1 \\ e_2 \\ 0 \\ 0 \\ 0 \\ 0 \end{bmatrix},$$

and

$$a_{11} = \frac{-2\left(C_r + C_f\right)}{Mv_x},\ a_{12} = -v_x + \frac{2\left(l_r C_r - l_f C_f\right)}{Mv_x},\ e_1 = \frac{1}{M},$$
$$a_{21} = \frac{2\left(l_r C_r - l_f C_f\right)}{I_z v_x},\ a_{22} = \frac{-2\left(l_r^2 C_r + l_f^2 C_f\right)}{I_z v_x},\ e_2 = \frac{l_w}{I_z},$$
$$T_{s1} = \frac{2C_f \eta_t}{I_s R_s^2 v_x},\ T_{s2} = \frac{2C_f l_f \eta_t}{I_s R_s^2 v_x},\ T_{s3} = \frac{-2C_f \eta_t}{I_s R_s^2},\ \lambda = \frac{1}{I_s R_s},$$
$$T_{s4} = \frac{-Bs}{I_s},\ b_1 = \frac{2C_f}{M},\ b_2 = \frac{2l_f C_f}{I_z},\ C_r = \kappa C_{r0},\ C_f = \kappa C_{f0}.$$

The state $x_v^\top = \begin{bmatrix} v_y & r & \psi_L & y_L & \delta & \dot{\delta} \end{bmatrix}$ of (1) is composed by the lateral velocity v_y, the yaw rate r, the heading error ψ_L, the lateral offset y_L from the road centerline at a look-ahead distance l_s, the steering angle δ and its time derivative $\dot{\delta}$. The lateral wind force $w = f_w$ is a system disturbance. For system (1), the driver torque T_d is measured whereas the assistance torque T_c has to be designed such that the studied LKAS can effectively share the vehicle control with human drivers.

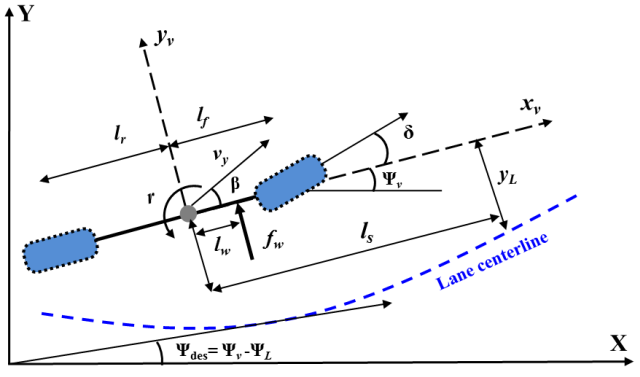

Fig. 1. Lateral vehicle behavior modeling.

TABLE I
VEHICLE MODEL PARAMETERS

Symbol	Description	Value
M	total mass of the vehicle	2025 kg
l_f	distance from gravity center to front axle	1.3 m
l_r	distance from GC to rear axle	1.6 m
l_w	distance from GC to wind impact center	0.4 m
l_s	look-ahead distance	5 m
η_t	tire length contact	0.13 m
I_z	vehicle yaw moment of inertia	2800 kgm^2
I_s	steering system moment of inertia	0.05 kgm^2
R_s	steering gear ratio	16
B_s	steering system damping	5.73
κ	adhesion coefficient	1
C_{f0}	front cornering stiffness	57000 N/rad
C_{r0}	rear cornering stiffness	59000 N/rad

B. Driver-in-the-Loop Vehicle Model

To improve the mutual understanding between the driver and the automation, the driver modeling should be integrated into the road-vehicle system for control purposes [9], [10].

It has been shown that for driving tasks, the driver is guided on the road by looking at two specific points called *near* point and *far* point [25]. These points can be characterized by two visual angles θ_{near} and θ_{far} which represent respectively the drivers' *compensatory* and *anticipatory* behaviors [8], [25]. For the compensatory control, based on the visual information in front of the vehicle (i.e. θ_{near}) the driver adjusts his/her torque applied on the wheel to obtain a desired lateral deviation with respect to the lane centerline. This behavior can be modeled by $\mathbf{G}_c = K_{d1}\theta_{near}$, where K_{d1} represents the driver's proportional action in accordance with θ_{near}. Concerning the anticipatory control, the driver uses the vision system to get the characteristics of the road ahead, in particular the change of its curvature. On this basis, s/he predicts the future vehicle trajectory and provides anticipative steering actions via the wheel before entering into the turn. The driver's anticipatory behavior is represented by $\mathbf{G}_a = K_{d2}\theta_{far}$, which generates a torque proportional to the *far* visual angle θ_{far}. As a result, the driver torque can be modeled as follows:

$$T_d = \mathbf{G}_c + \mathbf{G}_a = K_{d1}\theta_{near} + K_{d2}\theta_{far}. \tag{2}$$

Depending on the values of K_{d1} and K_{d2}, the corresponding driver gives more importance to compensatory and/or anticipatory controls. Here, these two gains representing the driver's style are identified with the data collected in our vehicle simulator. The two visual angles can be expressed by [8]:

$$\theta_{near} = \frac{y_L}{v_x T_p} + \psi_L, \quad \theta_{far} = \theta_1 v_y + \theta_2 r + \theta_3 \delta_d, \tag{3}$$
$$\theta_1 = \tau_a^2 a_{21}, \quad \theta_2 = \tau_a + \tau_a^2 a_{22}, \quad \theta_3 = \tau_a^2 b_2, \quad \delta_d = \delta R_s,$$

where T_p is the preview time and τ_a represents the anticipatory time. From (2)-(3), the driver torque can be rewritten as

$$\begin{aligned} &T_d = T_{d1} v_y + T_{d2} r + K_{d1}\psi_L + T_{d3} y_L + T_{d4}\delta, \\ &T_{d1} = K_{d2}\tau_a^2 a_{21}, \qquad T_{d2} = K_{d2}\left(\tau_a + \tau_a^2 a_{22}\right), \\ &T_{d3} = K_{d1}/\left(v_x T_p\right), \quad T_{d4} = K_{d2}\tau_a^2 b_2 R_s. \end{aligned} \tag{4}$$

Integrating (4) into (1), the driver-vehicle model is obtained

$$\dot{x}_v = A_v x_v + B T_c + B_w w, \tag{5}$$

where

$$A_v = \begin{bmatrix} a_{11} & a_{12} & 0 & 0 & b_1 & 0 \\ a_{21} & a_{22} & 0 & 0 & b_2 & 0 \\ 0 & 1 & 0 & 0 & 0 & 0 \\ 1 & l_s & v_x & 0 & 0 & 0 \\ 0 & 0 & 0 & 0 & 0 & 1 \\ \hat{T}_{s1} & \hat{T}_{s2} & \lambda K_{d1} & \lambda T_{d3} & \hat{T}_{s3} & T_{s4} \end{bmatrix},$$

and

$$\hat{T}_{s1} = T_{s1} + \lambda T_{d1}, \quad \hat{T}_{s2} = T_{s2} + \lambda T_{d2}, \quad \hat{T}_{s3} = T_{s3} + \lambda T_{d4}.$$

In this work, the state of system (5) can be measured for control design and real-time implementation.

III. COOPERATIVE CONTROL APPROACH FOR STEERING ASSISTANCE SYSTEM

This paper aims to propose a new control approach for a LKAS such that it can effectively share the control authority with a human driver to perform a driving task. For that, this shared control approach is based on two following studies.

1) The human-machine interaction guidelines in [11] show that the driver should: (i) always remain in the control loop; (ii) receive continuous feedback from the automation and continuously interact with it; (iii) take advantage of increased performance and reduced workload thanks to the LKAS.
2) The study on the need for assistance according to the driver's workload and performance in [26] indicates that the levels of assistance of the LKAS should be designed to relieve the driver in underload and overload conditions, see Fig. 2.

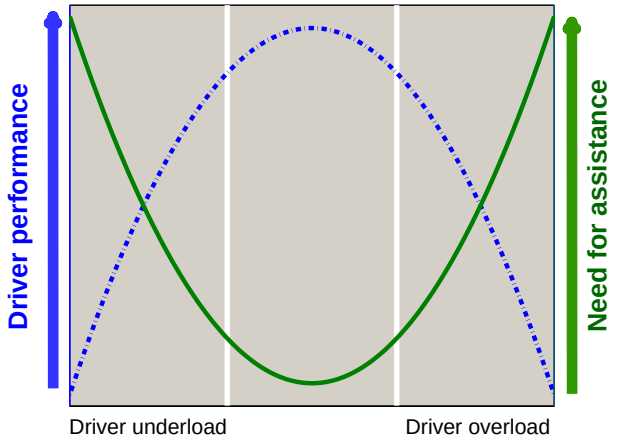

Fig. 2. U-shape function representing the need for assistance according to the driver's load and performance [26].

In order to meet the above design guidelines, we propose to modulate the assistance torque T_c in accordance with the real-time driving activity of the driver as follows:

$$T_c = \mu\left(\theta_d\right) u, \tag{6}$$

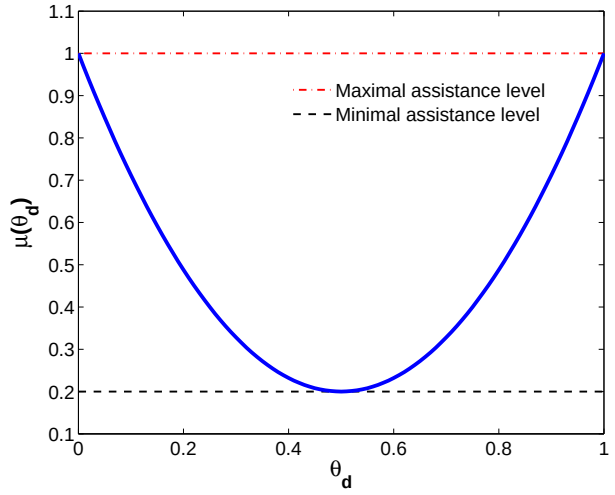

Fig. 3. Weighting function according to the driver activity variable with $\omega_1 = 0.32$, $\omega_2 = 0.5$ and $\mu_{\min} = 0.2$.

where the variable $\theta_d \in [0, 1]$ represents the driver's driving activity, and the fictive torque u will be designed. The weighting function $\mu(\theta_d)$ should allow the LKAS providing a continuous assistance to the driver according to his/her real-time driving activity. In this work, this time-varying term is of the following form:

$$\mu(\theta_d) = \omega_1 (\theta_d - \omega_2)^2 + \mu_{\min}, \tag{7}$$

where the parameters $\omega_1 = 3.2$, $\omega_2 = 0.5$ and $\mu_{\min} = 0.2$ are parameterized such that $\mu(\theta_d)$ represents the U-shape function characterizing the need for assistance of the driver shown in Fig. 2. Observe from Fig. 3 and the expression (6) that $T_c = u$ when the maximal assistance level is reached, i.e. $\mu(\theta_d) = \mu_{\max} = 1$. In addition, the minimal assistance level $\mu_{\min}$ is chosen such that the assistance torque T_c can benefit from a large variation range of $\mu(\theta_d)$, i.e. the real-time information on the driver's activity can be effectively exploited by the shared control strategy. However, unnecessarily small value of $\mu_{\min}$ could introduce some conservatism to the control problem.

In this work, the variable θ_d depends on two factors: (1) the driver torque, and (2) the real-time information on the driver state provided by the driver monitoring system [5]. This latter is used to verify if the driver is able to take the control of the vehicle for some specific maneuvers, or to make sure that the driver is not drowsy and s/he is aware of the driving situation. The information from the driver monitoring system is represented by a continuous variable $0 \leq \mathrm{DS} \leq 1$ ($\mathrm{DS} = 0$ when the driver is completely out of his/her driving capacity and $\mathrm{DS} = 1$ when s/he is fully aware of the driving situation). Notice that the driver activity variable θ_d is nonlinear by its nature since the driver's distraction increases *exponentially* with time when the driver looks away from the road scene (i.e. when s/he is distracted), but increases nearly instantaneously when s/he refocuses on the driving activity [5], [27]. Here, this driver's driving behavior is modeled as follows:

$$\theta_d = 1 - e^{-(\sigma_1 T_{dN})^{\sigma_2} \mathrm{DS}^{\sigma_3}}. \tag{8}$$

The normalized driver torque is given by $T_{dN} = \left| \frac{T_d}{T_{d\max}} \right|$, where $T_{d\max}$ is the maximal driver torque. The parameter $\sigma_1 = 2$ is used together with T_{dN} to represent the driver's involvement level in his/her driving tasks whereas the parameters $\sigma_2 = \sigma_3 = 3$ represent the degree of influence of the driver torque and the driver state on θ_d. These parameters are suitably chosen so that the driver can be *appropriately* assisted by the LKAS according to her/his real-time driving activity. Indeed, as can be observed in Fig. 4, when the driver torque and/or the driver state remain(s) small (which means that the driver's activity is not significant), the corresponding value of θ_d is small, thus a high level of assistance is required. When the driver is highly involved in the driving process, i.e. θ_d tends to 1 (for example when the driver need to realize a difficult maneuver), an important assistance from the LKAS is also required to help him/her. With a constant driver torque (respectively driver state), θ_d increases according to the driver state (respectively driver torque).

Remark 1. From the above discussions, notice that by (6), the proposed control approach allows to design the assistance torque T_c in accordance with the driver's need for assistance represented by the weighting function $\mu(\theta_d)$ in (7). This latter is, in turn, obtained in function of the driver's real-time activity defined by θ_d in (8). Therefore, the aforementioned guidelines on human-automation interaction can be directly considered in the control design with the new shared control approach.

From (5) and (6), the driver-in-the-loop vehicle model can be rewritten in the following form:

$$\dot{x}_v = A_v x_v + B_u u + B_w w, \tag{9}$$

where $B_u^\top = \begin{bmatrix} 0 & 0 & 0 & 0 & 0 & \lambda\mu(\theta_d) \end{bmatrix}$. Notice that since $\mu(\theta_d) > 0$, for $\theta_d \in [0, 1]$, the controllability of (9) is always guaranteed. Note also that the dynamics of (9) depends on two time-varying parameters v_x and $\mu(\theta_d)$. Moreover, as mentioned above, state and control input constraints should be *explicitly* considered in the control design to improve the driver's safety and comfort. The T-S fuzzy model-based control method developed in next section provides an effective framework to handle these control issues.

IV. Takagi-Sugeno Fuzzy Model-Based Control Design for Constrained Systems

This section details the control design for T-S fuzzy systems subject to both state and control input limitations.

Notation: In the sequel, the following notations are adopted for brevity. Ω_r denotes the number set $\{1, 2, \ldots, r\}$. I is the identity matrix of appropriate dimension. For a matrix X, $\mathrm{He}\, X = X + X^\top$ and $X > 0$ means that X is positive definite. The ith element of a vector u is denoted by $u_{(i)}$ and $X_{(i)}$ indicates the ith row of matrix X. For a matrix $P > 0$, denote $\mathcal{E}(P) = \{x : x^\top P x \leq 1\}$. The functions η_i, $i \in \Omega_r$, satisfy the convex sum property if $\eta_i \geq 0$ and $\sum_{i=1}^r \eta_i = 1$. For such functions with any argument θ, denote $Y_\theta = \sum_{i=1}^r \eta_i(\theta) Y_i$, $Z_{\theta\theta} = \sum_{i=1}^r \sum_{j=1}^r \eta_i(\theta) \eta_j(\theta) Z_{ij}$ where Y_i and Z_{ij} are matrices of appropriate dimensions.

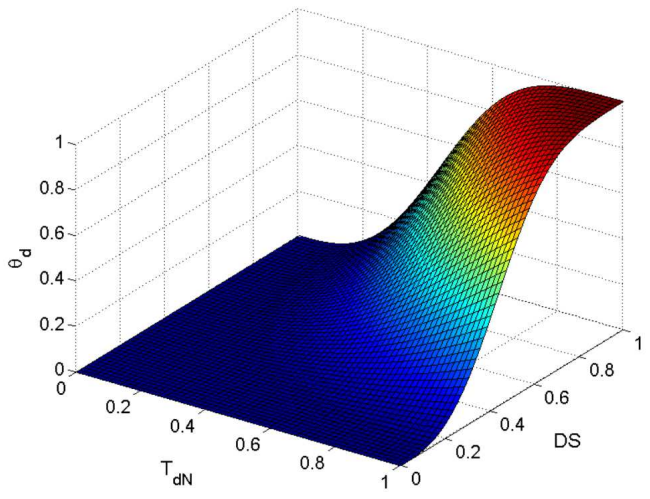

Fig. 4. Driver activity function θ_d with $\sigma_1 = 2$, $\sigma_2 = \sigma_3 = 3$.

A. Control Problem Formulation

Consider the following Takagi-Sugeno fuzzy system:

$$\begin{aligned} \dot{x} &= \sum_{i=1}^{r} \eta_i(\theta)\left(A_i x + B_i^u \operatorname{sat}(u) + B_i^w w\right) \\ z &= \sum_{i=1}^{r} \eta_i(\theta) C_i x \end{aligned} \tag{10}$$

where $x \in \mathbb{R}^{n_x}$ is the state, $u \in \mathbb{R}^{n_u}$ is the input, $w \in \mathbb{R}^{n_w}$ is the disturbance, $z \in \mathbb{R}^{n_z}$ is the performance output, $\theta \in \mathbb{R}^k$ is the vector of measured premise variables. The saturation function is defined as $\operatorname{sat}\left(u_{(l)}\right) = \operatorname{sign}\left(u_{(l)}\right) \min\left(\left|u_{(l)}\right|, u_{\max(l)}\right)$ where $u_{\max(l)}$, $l \in \Omega_{n_u}$, denotes the amplitude bound relative to the lth control input. The matrices of appropriate dimensions A_i, B_i^u, B_i^w, C_i, $i \in \Omega_r$, represent the set of r local linear systems and the membership functions $\eta_i(\theta)$ satisfy the convex sum property. For system (10), assume that the disturbance w is bounded in amplitude, i.e. it belongs to the set of functions $\mathcal{W}_\rho = \left\{w : \mathbb{R}^+ \mapsto \mathbb{R}^{n_w},\ w^\top w \le \rho,\ \rho > 0\right\}$.

Let us consider the parameter-dependent control law

$$u = \sum_{i=1}^{r} \eta_i(\theta) K_i x. \tag{11}$$

The control goal is to design the feedback gains K_i, $i \in \Omega_r$, such that (10) satisfies the following closed-loop properties.

i) **Property 1:** For $w = 0$, there exist a Lyapunov function $\mathbb{V}(x) = x^\top P x$, $P > 0$, and a positive scalar $\tau_1 > 0$ such that $\dot{\mathbb{V}}(x) < -\tau_1 \mathbb{V}(x)$ along the solution of (10) for any $x(0) \in \mathcal{E}(P)$.

ii) **Property 2:** For any $x(0) \in \mathcal{E}(P)$, the corresponding trajectory of (10) remains inside the polyhedral set of the state space described by

$$\mathcal{P}_x = \left\{x \in \mathbb{R}^{n_x} : \quad h_k^\top x \le 1, \quad k \in \Omega_q\right\}, \tag{12}$$

where the vectors $h_k \in \mathbb{R}^{n_x}$ are given.

iii) **Property 3:** For $\forall w \in \mathcal{W}_\rho$, $\rho > 0$, the closed-loop trajectories initialized in $\mathcal{E}(P)$ are required to stay in this set. Moreover, the $\mathcal{L}_\infty-$norm of the performance output is bounded, this is $z^\top z \le \gamma$ for some scalar $\gamma > 0$.

The following lemmas will be useful for the control design.

Lemma 1. [28] Given matrices $K_i, G_i \in \mathbb{R}^{n_u \times n_x}$, $i \in \Omega_r$, let us define the following set:

$$\mathcal{P}_u = \left\{x \in \mathbb{R}^{n_x} : \quad \left|\sum_{i=1}^{r} \eta_i \left(K_{i(l)} - G_{i(l)}\right) x\right| \le u_{\max(l)}\right\}$$

for $l \in \Omega_{n_u}$, and the dead-zone control input nonlinearity

$$\psi = u - \operatorname{sat}(u). \tag{13}$$

If $x \in \mathcal{P}_u$, then the following inequality holds

$$\psi^\top \left(\sum_{i=1}^{r} \eta_i S_i\right)^{-1} \left[\psi - \sum_{i=1}^{r} \eta_i G_i x\right] \le 0,$$

for any diagonal positive definite matrices $S_i \in \mathbb{R}^{n_u \times n_u}$ and scalar functions η_i, $i \in \Omega_r$, satisfying the convex sum property.

Remark 2. Lemma 1 presents an extension version of the generalized sector condition to deal with the control input nonlinearity proposed in [28]. This extension allows all involved matrices being parameter-dependent which contributes to reduce the design conservatism.

Lemma 2. [29] Let Ψ_{ij} and η_i, $i, j \in \Omega_r$ be respectively symmetric matrices of appropriate dimensions and a family of scalar functions satisfying the convex sum property. The condition $\sum_{i=1}^{r}\sum_{j=1}^{r} \eta_i \eta_j \Psi_{ij} < 0$ holds if

$$\begin{cases} \Psi_{ii} < 0, \quad i \in \Omega_r, \\ \dfrac{2}{r-1}\Psi_{ii} + \Psi_{ij} + \Psi_{ji} < 0, \quad i, j \in \Omega_r \text{ and } i > j. \end{cases} \tag{14}$$

B. LMI Design Conditions for Constrained T-S Systems

The following theorem allows for the design of a controller (11) that satisfies the above-mentioned closed-loop properties.

Theorem 1. Given T-S fuzzy system (10), positive scalars ρ and τ_1. If there exist positive definite matrix $X \in \mathbb{R}^{n_x \times n_x}$, diagonal positive definite matrices $S_i \in \mathbb{R}^{n_u \times n_u}$, matrices $X_{21}^i \in \mathbb{R}^{n_z \times n_x}$, $X_{22}^i \in \mathbb{R}^{n_z \times n_z}$, $X_{23}^i \in \mathbb{R}^{n_z \times n_u}$, $X_{31}^i \in \mathbb{R}^{n_u \times n_x}$, $X_{32}^i \in \mathbb{R}^{n_u \times n_z}$, $X_{33}^i \in \mathbb{R}^{n_u \times n_u}$, $V_i \in \mathbb{R}^{n_u \times n_x}$, $W_i \in \mathbb{R}^{n_u \times n_x}$, $i \in \Omega_r$, and positive scalars τ_2, γ satisfying (14) and

$$\begin{bmatrix} X & V_{i(l)}^\top - W_{i(l)}^\top \\ V_{i(l)} - W_{i(l)} & u_{\max(l)}^2 \end{bmatrix} > 0,\ i \in \Omega_r,\ l \in \Omega_{n_u} \tag{15}$$

$$\begin{bmatrix} X & X h_k \\ h_k^\top X & 1 \end{bmatrix} > 0, \quad k \in \Omega_p \tag{16}$$

$$\tau_1 - \tau_2 \rho > 0 \tag{17}$$

$$\begin{bmatrix} X & X C_i^\top \\ C_i X & \gamma I \end{bmatrix} \ge 0, \quad i \in \Omega_r \tag{18}$$

where the quantity Ψ_{ij} is defined as follows:

$$\Psi_{ij} = \operatorname{He}\begin{bmatrix} \Psi_{ij(1,1)} & B_i^u X_{32}^j & B_i^u X_{33}^j & -B_i^u S_j & B_i^w \\ \Psi_{ij(2,1)} & -X_{22}^j & -X_{23}^j & 0 & 0 \\ \Psi_{ij(3,1)} & -X_{32}^j & -X_{33}^j & 0 & 0 \\ W_i & 0 & 0 & -S_j & -S_j \\ 0 & 0 & 0 & 0 & -\tau_2 I/2 \end{bmatrix} \tag{19}$$

with $\Psi_{ij(1,1)} = A_i X + B_i^u X_{31}^j + \tau_1 X/2$, $\Psi_{ij(2,1)} = C_i X - X_{21}^j$, $\Psi_{ij(3,1)} = V_i - X_{31}^j$. Then, the parameter-dependent controller (11) with the feedback gains given by

$$K_i = V_i X^{-1}, \quad i \in \Omega_r, \tag{20}$$

solves the control problem stated in Section IV-A.

Proof. Define the augmented vector $\tilde{x}^\top = \begin{bmatrix} x^\top & z^\top & u^\top \end{bmatrix}$. Using the notations given at the beginning of Section IV and the expressions in (10) and (11), the closed-loop T-S system can be *equivalently* rewritten in the following augmented form:

$$\mathbb{E}\dot{\tilde{x}} = \mathbb{A}_\theta \tilde{x} + \mathbb{B}_\theta^w w - \mathbb{B}_\theta^\psi \psi, \tag{21}$$

where ψ is defined in (13) and

$$\mathbb{E} = \begin{bmatrix} I & 0 & 0 \\ 0 & 0 & 0 \\ 0 & 0 & 0 \end{bmatrix}, \qquad \mathbb{A}_i = \begin{bmatrix} A_i & 0 & B_i^u \\ C_i & -I & 0 \\ K_i & 0 & -I \end{bmatrix},$$
$$\mathbb{B}_i^w = \begin{bmatrix} B_i^{w\top} & 0 & 0 \end{bmatrix}^\top, \quad \mathbb{B}_i^\psi = \begin{bmatrix} B_i^{u\top} & 0 & 0 \end{bmatrix}^\top.$$

Let us introduce the following parameter-dependent matrix:

$$\mathbb{X}_\theta = \sum_{j=1}^{r} \eta_j(\theta) \begin{bmatrix} X & 0 & 0 \\ X_{21}^j & X_{22}^j & X_{23}^j \\ X_{31}^j & X_{32}^j & X_{33}^j \end{bmatrix}. \tag{22}$$

Since $X > 0$, it follows that

$$\mathbb{X}_\theta^\top \mathbb{E}^\top = \mathbb{E}\mathbb{X}_\theta = \begin{bmatrix} X & 0 & 0 \\ 0 & 0 & 0 \\ 0 & 0 & 0 \end{bmatrix} \geq 0. \tag{23}$$

By virtue of Lemma 2, the condition (14) implies clearly that

$$\Psi_{\theta\theta} = \sum_{i=1}^{r} \sum_{j=1}^{r} \eta_i(\theta)\, \eta_j(\theta)\, \Psi_{ij} < 0. \tag{24}$$

The inequality (24) implies that all diagonal sub-matrix blocks of $\Psi_{\theta\theta}$ are negative definite. Consequently, it follows that $\begin{bmatrix} X_{22}^\theta & X_{23}^\theta \\ X_{32}^\theta & X_{33}^\theta \end{bmatrix}$ is nonsingular, and so is $\mathbb{X}_\theta$ in (22) since $X > 0$. Denote $\mathbb{P}(\theta) = \mathbb{X}_\theta^{-1}$. Pre- and post- multiplying (23) with $\mathbb{P}(\theta)^\top$ and its transpose yields

$$\mathbb{E}^\top \mathbb{P}(\theta) = \mathbb{P}(\theta)^\top \mathbb{E} \geq 0. \tag{25}$$

Consider a candidate Lyapunov function of the following form:

$$\mathbb{V}(\tilde{x}) = \tilde{x}^\top \mathbb{E}^\top \mathbb{P}(\theta) \tilde{x}. \tag{26}$$

From the definitions of the augmented vector $\tilde{x}$, the matrix $\mathbb{E}$, and the relation (25), it follows that

$$\mathbb{V}(\tilde{x}) \equiv \mathbb{V}(x) = x^\top P x, \tag{27}$$

where $P = X^{-1}$. Notice that under the control law expression (11), the forms of Lyapunov functions (26) and (27), respectively closed-loop systems (10) and (21) are strictly *equivalent*. However, the use of (26) associated with (21) allows introducing the parameter-dependent matrices X_{21}^θ, X_{22}^θ, X_{23}^θ, X_{31}^θ, X_{32}^θ, X_{33}^θ (see (22)) into the design procedure. This aims to reduce the conservatism of the results [30].

Let $G_i = W_i X^{-1}$. Notice that (15) (respectively (16)) implies the inclusion $\mathcal{E}(P) \subset \mathcal{P}_u$ (respectively $\mathcal{E}(P) \subset \mathcal{P}_x$). Pre- and post- multiplying (24) with $\operatorname{diag}\left(\mathbb{X}_\theta^\top,\ S_\theta,\ I\right)$ and its transpose, it can be proved that (24), with Ψ_{ij} given in (19), is equivalent to the following condition:

$$\operatorname{He}\begin{bmatrix} \mathbb{P}(\theta)^\top \mathbb{A}_\theta + P^* & -\mathbb{P}(\theta)^\top \mathbb{B}_\theta^\psi & \mathbb{P}(\theta)^\top \mathbb{B}_\theta^w \\ G_{\theta\theta}^* & -S_\theta^{-1} & 0 \\ 0 & 0 & -\tau_2 I/2 \end{bmatrix} < 0 \tag{28}$$

with $P^* = \begin{bmatrix} \tau_1 P/2 & 0 & 0 \\ 0 & 0 & 0 \\ 0 & 0 & 0 \end{bmatrix}$ and $G_{\theta\theta}^* = \begin{bmatrix} S_\theta^{-1} G_\theta \\ 0 \\ 0 \end{bmatrix}$. Pre- and post- multiplying (28) by $\begin{bmatrix} \tilde{x}^\top & \psi^\top & w^\top \end{bmatrix}$ and its transpose, the following condition is obtained after some manipulations:

$$\dot{\mathbb{V}}(x) + \tau_1 x^\top P x - \tau_2 w^\top w - 2\psi^\top S_\theta^{-1} \left[\psi - G_\theta x\right] < 0 \tag{29}$$

Since $\mathcal{E}(P) \subset \mathcal{P}_u$, by Lemma 1, (29) implies clearly that

$$\dot{\mathbb{V}}(x) + \tau_1 x^\top P x - \tau_2 w^\top w < 0, \quad \forall x \in \mathcal{E}(P). \tag{30}$$

From now, two following cases can be distinguished.
i) **Case 1:** $w = 0$. It follows from (30) that for $\forall x \in \mathcal{E}(P)$, $\dot{\mathbb{V}}(x) < -\tau_1 x^\top P x$, which proves Property 1. This means that all trajectories of (10) initialized in $\mathcal{E}(P)$ converge asymptotically to the origin with a decay rate smaller than $\tau_1/2$.
ii) **Case 2:** $w \neq 0$, $w \in \mathcal{W}_\rho$. It follows from (17) and (30) that

$$\dot{\mathbb{V}}(x) + \tau_1 \left(x^\top P x - 1\right) + \tau_2 \left(\rho - w^\top w\right) < 0. \tag{31}$$

The condition (31) guarantees that the ellipsoid $\mathcal{E}(P)$ is a robustly positively invariant set [23] with respect to the closed-loop system (10). Furthermore, (18) implies that

$$\begin{bmatrix} X & C_\theta^\top \\ C_\theta & \gamma I \end{bmatrix} \geq 0. \tag{32}$$

By Schur complement lemma [24], it follows from (32) that

$$z^\top z = x^\top C_\theta^\top C_\theta x \leq \gamma x^\top P x \leq \gamma, \quad \forall x \in \mathcal{E}(P),$$

which means that the $\mathcal{L}_\infty-$norm of z is bounded $\|z\|_\infty^2 \leq \gamma$. These prove Properties 2, 3 and complete the proof. □

Remark 3. The LMI conditions in Theorem 1 can be easily solved with available numerical solvers [24]. In this work, the feedback gains K_i, $i \in \Omega_r$, in (20) are computed with SeDuMi solver and YALMIP toolbox [31].

Remark 4. The decay rate τ_1 in Property 1 is related to the closed-loop time performance [14]. A large value of this tuning parameter leads to a fast convergence time; however the corresponding controller could induce aggressive behaviors. In particular, this situation could get worst if the disturbance signal is involved in the system dynamics as the case of (9).

V. Application to Shared Lateral Control

Hereafter, the application of Theorem 1 to the vehicle shared control problem is highlighted.

A. T-S Representation of Driver-Vehicle System

For control purposes, the performance output z of (9) is defined such that it can represent the control performance in terms of both lane keeping and driving comfort:

$$z = \begin{bmatrix} a_y & \theta_{near} & \theta_{far} & \dot{\delta} \end{bmatrix}^\top. \tag{33}$$

Notice that the lane keeping performance is represented by *near* and *far* visual angles which allow to consider respectively the *compensatory* and *anticipatory* behaviors of the driver, see (3). The driving comfort is represented by the lateral acceleration $a_y \cong v_x r$. The steering rate $\dot{\delta}$ is introduced in (33) to guarantee a desired comfort for steering correction and to improve the vehicle damping response. Note that all components of z can be expressed by those of x_v in (9) as

$$z = \begin{bmatrix} 0 & v_x & 0 & 0 & 0 & 0 \\ 0 & 0 & 1 & \frac{1}{v_x T_p} & 0 & 0 \\ \theta_1 & \theta_2 & 0 & 0 & \theta_3 & 0 \\ 0 & 0 & 0 & 0 & 0 & 1 \end{bmatrix} x. \tag{34}$$

Remark that the system matrices of (9) and the performance matrix in (34) depend *nonlinearly* on the vehicle speed, i.e. v_x and $1/v_x$, and also on $\mu(\theta_d)$ which are measured and bounded $0.2 \leq \mu(\theta_d) \leq 1$, $v_{\min} \leq v_x \leq v_{\max}$ where $v_{\min} = 9$ and $v_{\max} = 25$. Moreover, using the first order Taylor's approximation, one has that

$$\frac{1}{v_x} = \frac{1}{v_0} + \frac{1}{v_1}\Delta_x, \quad v_x \cong v_0\left(1 - \frac{v_0}{v_1}\Delta_x\right), \tag{35}$$

where $\Delta_x \in [-1,\ 1]$ describes the variation of v_x between its lower and upper bounds. The constants in (35) are given by $v_0 = \frac{2v_{\min}v_{\max}}{v_{\min}+v_{\max}}$ and $v_1 = \frac{2v_{\min}v_{\max}}{v_{\min}-v_{\max}}$. Replacing (35) into (9), the premise vector of (9) can be defined as $\theta = \begin{bmatrix} \Delta_x & \mu(\theta_d) \end{bmatrix}^\top \in \mathbb{R}^2$. Using the sector nonlinearity approach [14], one can easily obtain $2^2 = 4$ linear models (A_i, B_i^u, B_i^w, C_i) and the corresponding membership functions $\eta_i(\theta)$, $i \in \Omega_4$, of the T-S model (10) of the driver-vehicle system (9). The details of these submodels and membership functions are not given here for brevity.

Remark 5. A natural choice of premise variables for (9) may be $\theta = \begin{bmatrix} v_x & 1/v_x & \mu(\theta_d) \end{bmatrix}^\top \in \mathbb{R}^3$. However, this leads to a T-S fuzzy model (10) with $2^3 = 8$ linear submodels when using the sector nonlinearity approach. In this paper, by (35) only Δ_x is used to represent the variation of both v_x and $1/v_x$. Therefore, the numerical complexity of the obtained T-S model is significantly reduced for control design and implementation.

Remark 6. In this paper, since the vehicle runs on a clean and dry road surface, the coefficient of adhesion is thus at its highest $\kappa = 1$, see Table I. However, the proposed T-S control method can be used to deal with the time-varying adhesion coefficient, i.e. $\kappa \in [\kappa_{\min}, 1]$ where $\kappa_{\min} > 0$. Note also that the dynamics matrix A in (1) already depends *linearly* on κ.

B. System Design Constraints

To improve the driver's safety and comfort, two categories of system constraints of (9) should be considered in the control design, i.e. state constraints and input limitations. For safety reasons, we take into account the "normal driving" zone which can be characterized by two following features [4].

1) The positions of the vehicle front wheels should be *simultaneously* located inside a strip $\pm d$ ($d = 1.5$ m) along the lane centerline during a normal lane keeping maneuver. This condition can be mathematically expressed as follows:
$$-\frac{(2d-a)}{2} \leq y_L + (l_f - l_s)\,\psi_L \leq \frac{(2d-a)}{2}, \tag{36}$$
where $a = 1.5$ m is the vehicle width.
2) The vehicle states should remain in a bounded state-space region given by
$$\begin{array}{lll} |v_y| \leq v_{y\max}, & |r| \leq r_{\max}, & |\psi_L| \leq \psi_{L\max}, \\ |y_L| \leq y_{L\max}, & |\delta| \leq \delta_{\max}, & \left|\dot{\delta}\right| \leq \dot{\delta}_{\max}. \end{array} \tag{37}$$

Following the guidelines in [4] and through our own experimental investigation, the following data are considered:

$$v_{y\max} = 1.5 \text{ m/s},\ r_{\max} = 0.55 \text{ rad/s},\ \psi_{L\max} = 0.1 \text{ rad},$$
$$y_{L\max} = 1 \text{ m},\ \delta_{\max} = 0.18 \text{ rad},\ \dot{\delta}_{\max} = 0.11 \text{ rad/s}.$$

Notice that the limitations on the steering rate $\dot{\delta}$ and the lateral acceleration a_y also improve the driver's comfort. Since one can be approximated that $a_y \cong v_x r$, the variation range of a_y is bounded by limiting the yaw rate r as in (37). Note also that the state constraints (36) and (37) can be straightforwardly reformulated in the form (12) for control purposes.

The input saturation can lead to control performance degradation or even makes the vehicle system unstable [22]. Therefore, as mentioned in Section I, the control input should be also limited to guarantee not only the driver's comfort but also the closed-loop stability during some specific maneuvers. In particular, this input limitation increases the driver's safety in case of assistance failure (i.e. the driver is able to compensate the assistance torque provided by the LKAS) [32]. Here, the control input constraint $u_{\max} = 6$ is the maximal torque of the steering system. After specifying all data of the vehicle T-S fuzzy model and its constraints, the assistance steering actions can be designed. Solving the LMI conditions in Theorem 1 leads to the following control gains of (11):

$$\begin{aligned} K_1 &= \begin{bmatrix} -63.8 & -119.9 & -558.1 & -10.9 & 14.2 & -12.7 \end{bmatrix}, \\ K_2 &= \begin{bmatrix} -37.9 & -65.3 & -119.9 & 3.7 & 277.5 & 16.5 \end{bmatrix}, \\ K_3 &= \begin{bmatrix} -11.4 & -59.7 & -679.2 & -46.5 & -205.1 & -52.4 \end{bmatrix}, \\ K_4 &= \begin{bmatrix} -3.5 & -14.2 & -148.2 & -11.5 & 290.1 & 13.4 \end{bmatrix}. \end{aligned}$$

Observe that the feedback gains corresponding to 4 linear submodels of the T-S fuzzy system are significantly different. This also justifies *a posteriori* the interest of the T-S model-based control method to improve the closed-loop performance.

VI. Hardware Experiments

In this section, the practical performance of the proposed shared controller is verified via a series of experiments conducted with a human driver and a SHERPA driving simulator. This interactive dynamic simulator is in the form of a Peugeot 206 vehicle fixed on a Stewart platform, see Fig. 5. This advanced simulator is structured around a SCANeR network connecting fifteen PC-type workstations. The whole software of the SHERPA simulator is developed with RTMaps environment composed by several modules which are in charge

of different tasks: perception, planning, driver monitoring, human-machine interface. It is also equipped with a Continental driver monitoring system which indicates the driver state. Notice that for the control design, a preliminary validation study of the driver-vehicle model (5) with experimental data collected from the SHERPA simulator has been carried out. Fig. 6 shows an overview of the control structure implemented in the SHERPA simulator. The "Driver activity analysis" unit aims at providing an appropriate weighting function $\mu(\theta_d)$ to compute the assistance torque T_c in accordance with the real-time behaviors of the driver, see Section III.

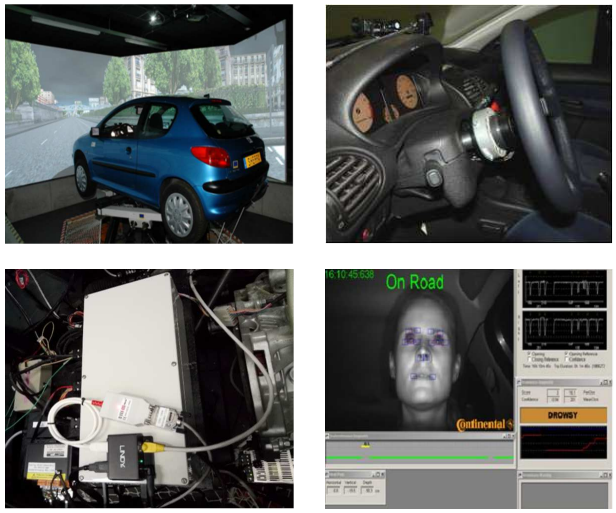

Fig. 5. SHERPA simulator (upper left). Steering system (upper right). Data acquisition system (bottom left). Continental driver monitoring system (bottom right).

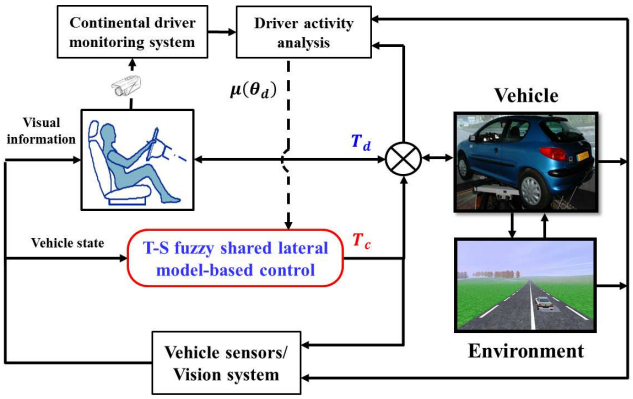

Fig. 6. Control structure implemented in the SHERPA interactive dynamic driving simulator.

A. Disturbance Rejection

For this scenario, the vehicle is on a straight road with $v_x = 15$ m/s and subject to an important wind disturbance $f_w = 1100$ N, see Fig. 7(a). This wind force generates a yaw moment disturbance which can be felt by the driver through the steering system. Since the vehicle system is *open-loop unstable*, therefore without any control the vehicle has naturally unstable behaviors in the presence of wind disturbance. To point out the performance of the proposed T-S fuzzy control method, three following cases are considered for this test.

- Case 1: *Automatic control*. The driver releases the steering wheel (i.e. $T_d = 0$) and the LKAS *solely* controls the vehicle.
- Case 2: *Manual control*. The vehicle is *manually* controlled by the driver *without* any assistance from the LKAS (i.e. $T_c = 0$).
- Case 3: *Shared control*. The LKAS shares the vehicle control with the driver to perform the lane keeping task.

Fig. 7 shows the comparison of vehicle responses obtained with three above cases. Observe in Fig. 7(b) that for all three cases, the same steering torques are required to reject effectively the undesirable wind effect. The corresponding lateral accelerations and tracking errors remain small, see respectively Figs. 7(c), (e) and (f). In Case 1, the T-S fuzzy controller offers the best control performance with smallest tracking errors. Notice also that compared to Case 2, better performance can be achieved with Case 3 where the LKAS and the driver *jointly* counteract the wind disturbance without generating conflict situation, see Fig. 7(d). Moreover, the driver only provides a part (about 50%) of the required torque in Case 3. This test scenario confirms clearly the effectiveness of the T-S controller and the shared control method in terms of disturbance rejection.

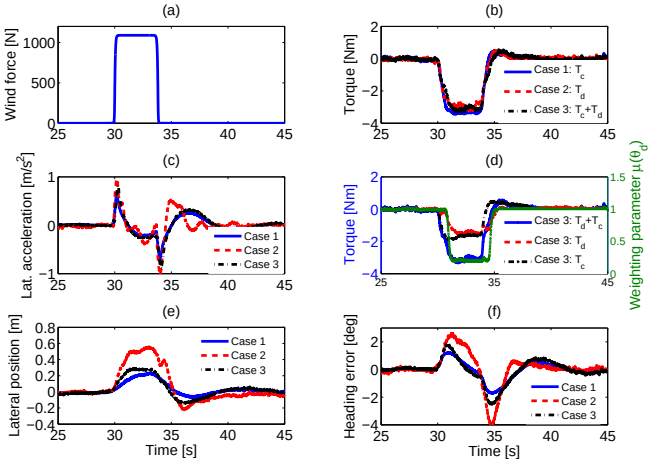

Fig. 7. Disturbance rejection performance. Case 1: automatic control, Case 2: manual control, Case 3: shared control.

B. Driving Task with Adaptive Level of Assistance

This scenario aims to point out the performance of the proposed shared controller according to the driver's need for assistance. For that, the lane keeping task is performed in four phases with the vehicle trajectory and speed given in Figs. 8(a) and (c). Phase 1 (from $10s$ to $40s$) corresponds to the lane keeping of the LKAS in the first curve (see Fig. 8(a)) *without* the intervention of the human driver. During this phase, the driver releases his hands from the steering wheel (i.e. $T_d = 0$) and the vehicle is *solely* controlled by the LKAS. As expected, Fig. 8(b) shows that in this situation $\mu(\theta_d) = 1$

which means obviously that the maximal level of assistance is required. Both controller and driver share the vehicle control to perform the driving task in Phase 2 (from $40s$ to $60s$). For Phase 3 (from $60s$ to $70s$), the driver is highly involved in the driving process (θ_d tends to 1); and the steering system provides thus an important assistance ($\mu(\theta_d)$ tends also to 1) to help him. This situation corresponds to the zone of driver overload depicted in Fig. 2. In Phase 4 (from $70s$ to $100s$), the assistance system provides almost the same amount of torque as the driver to help him to negotiate a difficult curve. It is also observed in Fig. 9 that the state constraints (37) are respected during the whole test.

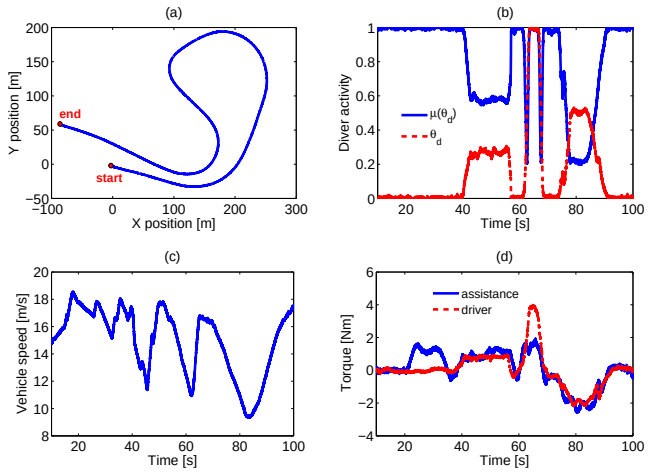

Fig. 8. Driving task with adaptive level of assistance.

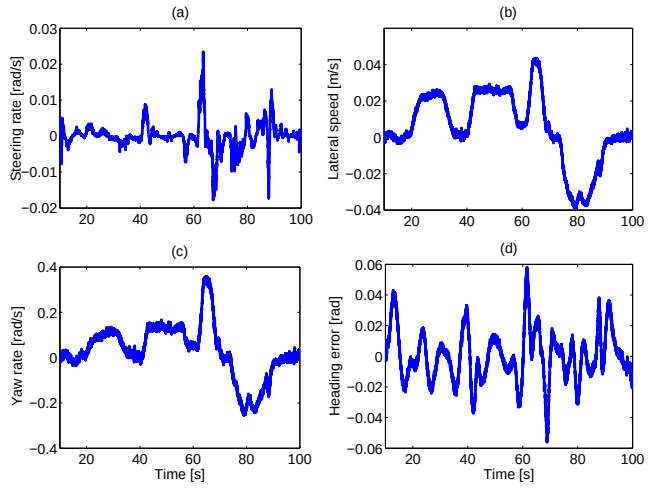

Fig. 9. Vehicle states corresponding to the results in Fig. 8.

C. Emergency Double Lane Change Maneuver

For this test, it is assumed that the driver desires to perform an *unexpected* double lane change maneuver to avoid two obstacles which are *not* detected by the automation. Notice that the driver-automation conflict arises naturally in this case since their driving goals are different, namely obstacle avoidance for the driver and lane keeping for the automation. To evaluate the performance of the proposed shared controller in terms of conflict management, two following cases are examined where two similar double lane change maneuvers are performed at the same vehicle speed $v_x = 20$ m/s, see Fig. 10-top.

- Case 1: Double lane change with an *adaptive* control authority allocation, i.e. the weighting function $\mu(\theta_d)$ in (7) is variable in accordance with the driver's real-time activity.
- Case 2: Double lane change with a constant control authority, e.g. the maximal level of assistance $\mu(\theta_d) = 1$.

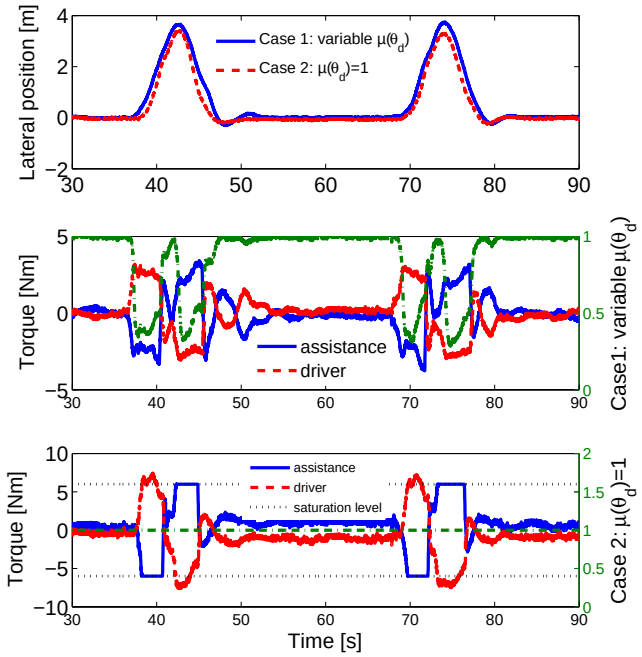

Fig. 10. Shared control with double lane change maneuver.

Fig. 10-middle (respectively -bottom) depicts the steering torques of both driving actors and the weighting function $\mu(\theta_d)$ obtained with Case 1 (respectively Case 2). Observe that in Case 1 the assistance torque T_c is computed according to the driver's activity so that he can easily realize the driving objective, i.e. only a small T_d is needed in this case. However, without considering the driver's real-time driving activity in the computation of T_c, the driver performs the same maneuver with difficulty in Case 2 since he must provide an important effort to compensate the large amount of saturated assistance torque. Moreover, the results of Case 2 also shows that in some specific situations, the control input u (and thus T_c) may tend easily to be saturated. Therefore, LMI-based design method for constrained T-S systems proposed in Section IV is obviously useful to guarantee the closed-loop stability in such situations.

To characterize the quality of the driver-automation shared control, the following energy indicators are used:

$$\mathcal{E}_d = \int_{t_1}^{t_2} T_d^2 dt, \quad \mathcal{E}_c = \int_{t_1}^{t_2} T_c^2 dt. \tag{38}$$

The numerical quantities $\mathcal{E}_d$ and $\mathcal{E}_c$ in (38) represent respectively the energy efforts delivered by the driver and the LKAS

during a time interval $[t_1,\ t_2]$. Notice that it is desirable from the viewpoint of *acceptability* (respectively *security*) that the driver (respectively the LKAS) provides an effort as small as possible to perform a given driving task [32]. Let us also define the *level of sharing* between the driver and the automation as

$$\mathcal{I}_{share} = \frac{\mathcal{E}_c}{\mathcal{E}_d}. \tag{39}$$

Three special cases can be noticed from (39): $\mathcal{I}_{share} = 0$ if there is no assistance, $\mathcal{I}_{share} = 1$ if the automation provides the same energy effort as the driver, and $\mathcal{I}_{share} > 1$ if the energy effort of the automation is greater than that of the driver. Observe in Table II that for the same double lane change with a similar level of sharing (about 90%), the values of both energy indicators in Case 1 are significantly lower than those of Case 2. This means that with the adaptive control authority allocation, the driver (and also the LKAS) provides less effort to perform the given maneuver. Therefore, the driver's comfort can be improved with the proposed shared control method.

TABLE II
COMPARISON OF SHARED CONTROL QUALITY

Energy indicator	$\mathcal{E}_d$ [N^{2}m^{2}s]	$\mathcal{E}_c$ [N^{2}m^{2}s]	$\mathcal{I}_{share}$ [%]
Case 1	107.23	98.89	92.22
Case 2	516.07	466.65	90.42

D. Obstacle Avoidance with Full Automatic Control

Suppose now that the vehicle should *solely* perform a lane change maneuver to avoid an obstacle which is detected by the vision system. For this, the standardized chicane test (see Fig. 11) is used to verify the practical performance of the proposed controller under highly dynamic maneuvering. Notice that for this test scenario, one has $T_d = 0$, $\theta_d = 0$, and $\mu(\theta_d) = 1$.

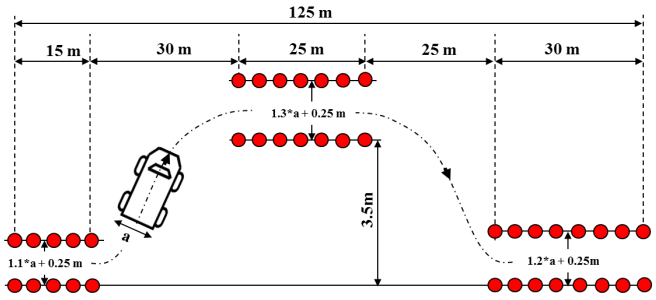

Fig. 11. Standardized chicane test scenario.

The vehicle responses obtained with the designed T-S fuzzy controller for chicane tests with three speeds: $v_x = 35$ km/h, $v_x = 45$ km/h and $v_x = 60$ km/h, are shown in Fig. 12. As expected, the controller provides more important effort to perform the same lane change maneuver when the speed increases. However, since the variation of vehicle speed is *explicitly* taken into account in the control design, robust stability of the vehicle for three chicane tests can be guaranteed with the proposed controller. Note also that the vehicle responses are quite similar under three different speeds. Moreover, for all chicane tests, variables representing the lane following performance of the vehicle remain in their predefined ranges which means that the vehicle performs *successfully* the standardized lane change maneuver in the absence of the human driver's action, see for example the yaw rates and the sideslip angles corresponding to these tests in Figs. 12(c) and (d).

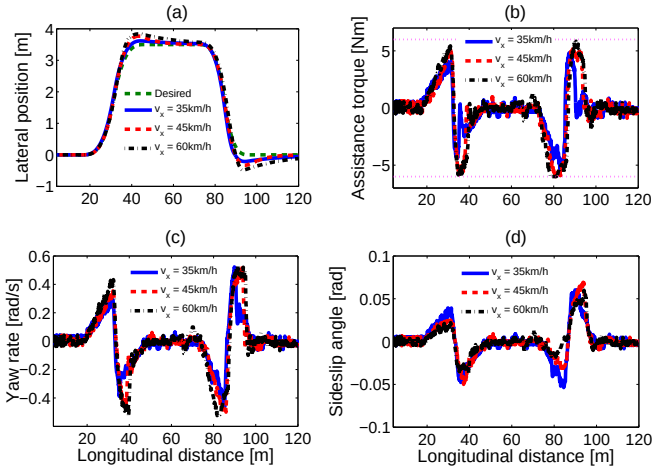

Fig. 12. Vehicle responses under the chicane test scenario.

VII. CONCLUDING REMARKS

In this paper, a new driver-automation cooperative approach has been proposed to deal with the shared lateral control of LKAS devices. By introducing a measured weighting parameter into the road-vehicle system, the assistance control actions can be designed in accordance with the real-time driving activity of drivers. Consequently, the conflicts between the driver and the automation can be effectively managed. T-S fuzzy model-based control method has been used to handle the time-varying driver activity parameter and also the vehicle speed variation. In particular, both state and control input limitations are *explicitly* considered in the control procedure with the proposed LMI-based design conditions. This aims to improve the driver's safety and comfort. The closed-loop stability and performance of the driver-vehicle system are rigorously proved using Lyapunov arguments. Experiments conducted with a human driver and an advanced driving simulator under various test scenarios have clearly demonstrated the effectiveness of the new control method. Future works focus on intensive human-factor experiments to further evaluate the *acceptability* of the proposed method for a large panel of drivers.

REFERENCES

[1] L. Li, D. Wen, N.-N. Zheng, and L.-C. Shen, "Cognitive cars: A new frontier for ADAS research," *IEEE Trans. Intell. Transp. Syst.*, vol. 13, no. 1, pp. 395–407, Mar. 2012.
[2] J. Navarro, F. Mars, and M. Young, "Lateral control assistance in car driving: Classification, review and future prospects," *IET Intel. Transport Syst.*, vol. 5, no. 3, pp. 207–220, Jun. 2011.
[3] R. Rajamani, *Vehicle Dynamics and Control*. Boston, Springer, 2012.
[4] N. Enache, M. Netto, S. Mammar, and B. Lusetti, "Driver steering assistance for lane departure avoidance," *Control Eng. Pract.*, vol. 17, no. 6, pp. 642–651, Jun. 2009.

[5] Y. Dong, Z. Hu, K. Uchimura, and N. Murayama, "Driver inattention monitoring system for intelligent vehicles: A review," *IEEE Trans. Intell. Transp. Syst.*, vol. 12, no. 2, pp. 596–614, Dec. 2011.
[6] A.-T. Nguyen, C. Sentouh, J. C. Popieul, and B. Soualmi, "Shared lateral control with on-line adaptation of the automation degree for driver steering assist system: A weighting design approach," in *54th IEEE Conf. on Decis. and Control*, pp. 857–862, Dec. 2015.
[7] X. Na and D. J. Cole, "Linear quadratic game and non-cooperative predictive methods for potential application to modelling driver-AFS interactive steering control," *Veh. Syst. Dyn.*, vol. 51, no. 2, pp. 165–198, Aug. 2013.
[8] C. Sentouh, B. Soualmi, J.-C. Popieul, and S. Debernard, "Cooperative steering assist control system," in *IEEE Int. Conf. on Syst., Man, and Cybern.*, pp. 941–946, Manchester, UK, Oct. 2013.
[9] L. Saleh, P. Chevrel, F. Claveau, J.-F. Lafay, and F. Mars, "Shared steering control between a driver and an automation: Stability in the presence of driver behavior uncertainty," *IEEE Trans. Intell. Transp. Syst.*, vol. 14, no. 2, pp. 974–983, Mar. 2013.
[10] B. Soualmi, C. Sentouh, J. Popieul, and S. Debernard, "Automation-driver cooperative driving in presence of undetected obstacles," *Control Eng. Pract.*, vol. 24, pp. 106–119, Mar. 2014.
[11] D. A. Abbink, M. Mulder, and E. R. Boer, "Haptic shared control: smoothly shifting control authority?" *Cogn., Technol. & Work*, vol. 14, no. 1, pp. 19–28, Nov. 2012.
[12] A. Franchi, C. Secchi, M. Ryll, H. H. Bülthoff, and P. R. Giordano, "Shared control: Balancing autonomy and human assistance with a group of quadrotor UAVs," *IEEE Rob. & Autom. Mag.*, vol. 19, no. 3, pp. 57–68, Sep. 2012.
[13] Y. Li, K. P. Tee, W. L. Chan, R. Yan, Y. Chua, and D. K. Limbu, "Continuous role adaptation for human-robot shared control," *IEEE Trans. on Rob.*, vol. 31, no. 3, pp. 672–681, Jun. 2015.
[14] K. Tanaka and H. Wang, *Fuzzy Control Systems Design and Analysis: a Linear Matrix Inequality Approach*. John Wiley & Sons, 2004.
[15] P. Qi, C. Liu, A. Ataka, H. K. Lam, and K. Althoefer, "Kinematic control of continuum manipulators using a fuzzy-model-based approach," *IEEE Trans. Ind. Electron.*, vol. 63, no. 8, pp. 5022–5035, Aug. 2016.
[16] C. Geng, L. Mostefai, M. Denai, and Y. Hori, "Direct yaw-moment control of an in-wheel-motored electric vehicle based on body slip angle fuzzy observer," *IEEE Trans. Ind. Electron.*, vol. 56, no. 5, pp. 1411–1419, May. 2009.
[17] A.-T. Nguyen, M. Dambrine, and J. Lauber, "Lyapunov-based robust control design for a class of switching non-linear systems subject to input saturation: Aapplication to engine control," *IET Control Theory & Appl.*, vol. 8, pp. 1789–1802, Jan. 2014.
[18] Q. Jia, W. Chen, Y. Zhang, and H. Li, "Fault reconstruction and fault-tolerant control via learning observers in Takagi-Sugeno fuzzy descriptor systems with time delays," *IEEE Trans. Ind. Electron.*, vol. 62, no. 6, pp. 3885–3895, Feb. 2015.
[19] J.-X. Xu, Z.-Q. Guo, and T. H. Lee, "Design and implementation of a Takagi-Sugeno fuzzy logic controller on a two-wheeled mobile robot," *IEEE Trans. Ind. Electron.*, vol. 60, no. 12, pp. 5717–5728, Nov. 2013.
[20] Y.-W. Liang, S.-D. Xu, D.-C. Liaw, and C.-C. Chen, "A study of T-S model-based SMC scheme with application to robot control," *IEEE Trans. Ind. Electron.*, vol. 55, no. 11, pp. 3964–3971, Sep. 2008.
[21] K. Tanaka, K. Yamauchi, H. Ohtake, and H. O. Wang, "Sensor reduction for backing-up control of a vehicle with triple trailers," *IEEE Trans. Ind. Electron.*, vol. 56, no. 2, pp. 497–509, Aug. 2009.
[22] S. Tarbouriech, G. Garcia, J. Gomes da Silva Jr., and I. Queinnec, *Stability and Stabilization of Linear Systems with Saturating Actuators*. London: Springer-Verlag, 2011.
[23] F. Blanchini, "Set invariance in control," *Automatica*, vol. 35, no. 11, pp. 1747–1767, Nov. 1999.
[24] S. Boyd, L. El Ghaoui, E. Feron, and V. Balakrishnan, *Linear Matrix Inequalities in System and Control Theory*. Philadelphia: SIAM, 1994.
[25] D. D. Salvucci and R. Gray, "A two-point visual control model of steering," *Perception*, vol. 33, no. 10, pp. 1233–1248, Dec. 2004.
[26] F. Flemisch, F. Nashashibi, N. Rauch, A. Schieben, S. Glaser, G. Temme, P. Resende *et al.*, "Towards highly automated driving: Intermediate report on the HAVEit-joint system," in *3rd European Road Transport Research Arena*, Brussels, Belgium, Jun. 2010.
[27] J. Pohl, W. Birk, and L. Westervall, "A driver-distraction-based lane-keeping assistance system," *Proc. Inst. Mech. Eng. I J. Syst. Control Eng.*, vol. 221, no. 4, pp. 541–552, Nov. 2007.
[28] A.-T. Nguyen, T. Laurain, R. Palhares, J. Lauber, C. Sentouh, and J.-C. Popieul, "LMI-based control synthesis of constrained Takagi-Sugeno fuzzy systems subject to $\mathcal{L}_2$ or $\mathcal{L}_\infty$ disturbances," *Neurocomputing*, vol. 207, pp. 793–804, Sep. 2016.
[29] H. Tuan, P. Apkarian, T. Narikiyo, and Y. Yamamoto, "Parameterized linear matrix inequality techniques in fuzzy control system design," *IEEE Trans. Fuzzy Syst.*, vol. 9, no. 2, pp. 324–332, Aug. 2001.
[30] K. Tanaka, H. Ohtake, and H. O. Wang, "A descriptor system approach to fuzzy control system design via fuzzy Lyapunov functions," *IEEE Trans. Fuzzy Syst.*, vol. 15, no. 3, pp. 333–341, Jun. 2007.
[31] J. Löfberg, "YALMIP: A toolbox for modeling and optimization in MATLAB," in *IEEE Int. Symp. on Comput. Aided Control Syst. Des.*, pp. 284–289, Taipei, Sep. 2004.
[32] J. P. Switkes, "Hand wheel force feedback with lane keeping assistance: combined dynamics, stability and bounding," Ph.D. dissertation, Stanford University, Nov. 2006.

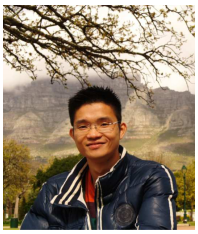

Anh-Tu Nguyen was born in a small town in the Middle of Vietnam, near Danang. He received both Engineering and MSc degrees in 2009 from Grenoble Institute of Technology, France, and his PhD degree in Control Engineering in 2013 from the University of Valenciennes, France.

After working a short period in 2010 at the French Institute of Petroleum, he began his doctoral program at the CNRS laboratory LAMIH in collaboration with VALEO Group. He was a postdoctoral researcher at the same laboratory from February 2014 to May 2016. Sine June 2016, he is a postdoctoral researcher at the CNRS laboratory IRCCyN. His research interests include LMI-based robust control and observation, constrained systems, fuzzy control systems, human-machine shared control with strong emphasis on vehicle engineering applications.

Chouki Sentouh was born in Jijel, Algeria. He received the MSc degree in Automatic Control from the University of Versailles, France in 2003 and his PhD degree in Automatic Control from the University of Évry, France, in 2007.

He was a postdoctoral researcher at the CNRS laboratory IRCCyN, France, from 2007 to 2009. Since 2009, he is an Associate Professor at the University of Valenciennes in LAMIH-UMR CNRS 8201. His research fields include automotive control, driver assistance systems with driver interaction, human driver modeling and cooperation in intelligent transportation systems. He is interested in shared control approaches to design assistance systems that can adapt their behavior according to the level of automation and the interaction with human driver.

Jean-Christophe Popieul is Professor in Automatic Control at the University of Valenciennes in LAMIH-UMR CNRS 8201. Since 1994 his main area of interest is in Transport Safety. He first focused on driver status assessment and led several studies dealing with driver vigilance and workload in collaboration with automakers and insurance companies. In 2004 he started to work on ADAS. Beginning with longitudinal driver assistance, he is now working on control sharing for full driving automation. Specialized in Human Centered Automation, he participated in many collaborative projects such as PREDIT ARCOS, CISIT, ANR ABV and D4S. He is currently the coordinator of the ANR CoCoVeA project and ELSAT 2020 project (350 researchers involved). He is a member of several scientific boards (ANR, PREDIT, i-Trans competitivity cluster, IRT Railenium). He is also at the head of the Interactive Simulation Platforms of the LAMIH-CNRS: SHERPA driving simulator, PSCHITT-Rail train/tramway simulator and PSCHITT-PMR wheelchair simulator.

View publication stats